Water-saturated mesoporous MCM-41 systems characterized by 1H NMR

ARTICLE *in* THE JOURNAL OF PHYSICAL CHEMISTRY A · FEBRUARY 1994

Impact Factor: 2.69 · DOI: 10.1021/j100058a034

4 AUTHORS, INCLUDING:

Eddy Walther. Hansen
University of Oslo
112 PUBLICATIONS **1,475** CITATIONS

SEE PROFILE

Water-Saturated Mesoporous MCM-41 Systems Characterized by ^1H NMR

Duncan Akporiaye, Eddy Walther Hansen,* Ralf Schmidt, and Michael Stöcker

SINTEF-SI, P.O. Box 124, Blindern 0314 Oslo, Norway

Received: August 31, 1993; In Final Form: October 26, 1993®

^1H NMR measurements on a new family of mesoporous molecular sieves, designated MCM-41, saturated with water show abrupt changes in the signal intensity of the water signal at specific temperatures, denoted as transition temperatures. A model equation is presented describing the intensity vs temperature behavior. Similar transition phenomena are also observed in line width vs temperature. A linear relationship between the spin–lattice relaxation rate (at −10 °C) and the first transition temperature, as determined from the intensity measurements, is found. This behavior is expected if it is assumed that the transition temperature can be predicted by Kelvin's equation and that the spin–lattice relaxation rate is proportional to the inverse of the pore radius, as previously reported in the literature.

Introduction

With reference to a recent publication by Overloop et al.[1] on freezing phenomenon in adsorbed water of high-surface-area materials such as silica gel, controlled-pore glass, and activated charcoal studied by NMR, our object with this short communication is to present a similar ^1H NMR study of a new family of mesoporous molecular sieves, designed as MCM-41 materials. These materials were recently discovered by researchers from the Mobil Oil Co.[2-4] These novel materials possess a hexagonal array of uniform, one-dimensional mesopores, varying in size from around 16 to 100 Å. They are synthesized from aluminosilicate gels using quaternary ammonium surfactants ($C_nH_{2n+1}(CH_3)_3N^+$) with different alkyl chain lengths (n = 8–16). It has been suggested that these mesoporous molecular sieves form through a liquid crystal templating mechanism, allowing the systematic preparation of uniform pore sizes within a defined range.[2] From this viewpoint, these materials are well suited to perform a rigorous investigation by NMR of the freezing phenomenon on a molecular level of different liquids restricted to small, well defined volumes.

Another object with this presentation is to examine if the signal intensity vs temperature data of the confined pore water can be correlated with other ^1H NMR parameters such as the line width and the spin–lattice relaxation time. Moreover, a mathematical expression for the NMR signal intensity of the pore water vs temperature will be presented.

Experimental Section

Three mesoporous MCM-41 materials, denoted in the following discussion by the letters A, B, and C, were saturated with water and studied by ^1H NMR in the temperature range −100 °C to room temperature. The accuracy of the temperature determination was within ±0.5 °C. A Varian VXR 300 S NMR spectrometer, operating at 300 MHz proton resonance frequency, was used. A bandwidth of 100 kHz and an acquisition time of 0.125 s were applied. Each spectrum was composed of 16 transients. Due to the short spin–lattice relaxation times, a pulse repetition time of 3 s was sufficient. The sample was temperature equilibrated for 10 min at each temperature before any measurements were performed. The spectra were accumulated applying a temperature cycling, i.e., heating and cooling of the sample.

We noted at the end of the experimental session that the pulse angle was set to approximately 5 μs, corresponding to a pulse angle of 22.5°. It should be emphasized that a 90° pulse angle could have been successfully applied, thus improving the S/N ratio. However, the shorter pulse angle chosen in these experiments has no effect on the quantitative interpretation of the data. The intensity (integral) and line width of the NMR signal of the mobile water confined in the pores were monitored as a function of temperature.

In this report the line width of the absorption signal at half height ($\Delta\nu_{1/2}$) is reported as an *apparent* spin–spin relaxation rate ($1/T_2$) by applying eq 1, implicitly assuming a Lorentzian line shape.

$$1/T_2 = \pi\Delta\nu_{1/2} \tag{1}$$

Measurement of the true spin–spin relaxation time is in progress and will be reported in the near future.

The spin–lattice relaxation time (T_1) for the confined pore water has been measured at −10 °C by applying an inversion recovery pulse sequence. The reason for determining the relaxation time at this temperature is that water at the outer surface of the sample is frozen under these conditions and thus will not affect the T_1 of the pore water. Moreover, no pore water is frozen out at this temperature for the samples investigated.

The materials investigated were synthesized according to a procedure given by Beck et al.[2] using octyltrimethyl- (sample C) and tetradecyltrimethylammonium bromide (sample B). The addition of mesitylene (sample A) allowed materials with pores >40 Å to be obtained. Synthesis time of 144 h and a synthesis temperature of 100 °C were applied. All syntheses were performed in Teflon bottles and the samples were thoroughly washed with distilled water and dried under ambient conditions. The remaining template was removed by calcination at 540 °C for 1 h in flowing nitrogen, followed by 6 h in flowing air at the same temperature.

Results and Discussion

The general behavior of the signal intensity of the mobile water—confined in a mesopore system—vs temperature is depicted in Figure 1 (sample A, pore size of approximately 50 Å). The solid (warming)/dotted (cooling) lines are model calculations and will be discussed briefly, in the Appendix.

A typical characteristic of these plots is a "stepwise" reduction in intensity with decreasing temperature. The intensity vs temperature shows a decrease with decreasing temperature which occurs at a lower temperature on cooling than on rewarming. This hysteresis effect is typical for a freezing phenomenon in which part of the water becomes ice. Two such "discontinuities" in the intensity vs inverse temperature are observed, at approximately 0 °C and at −29 °C (the average of the temperature

* To whom correspondence should be addressed.

® Abstract published in *Advance ACS Abstracts,* January 15, 1994.

0022-3654/94/2098-1926$04.50/0

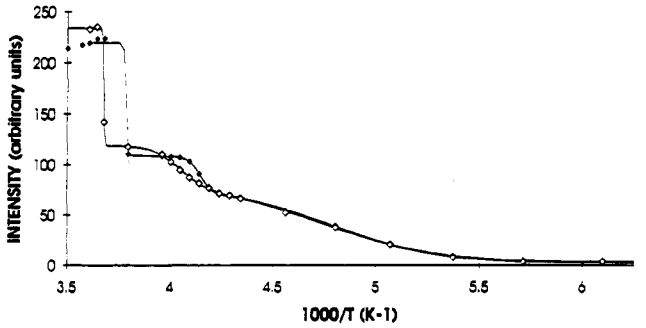

Figure 1. ^{1}H NMR signal intensity of the pore water vs inverse temperature of sample A. Solid lines represents model calculations (eq A6). (◇) Cooling of the sample. (◆) Heating of the sample.

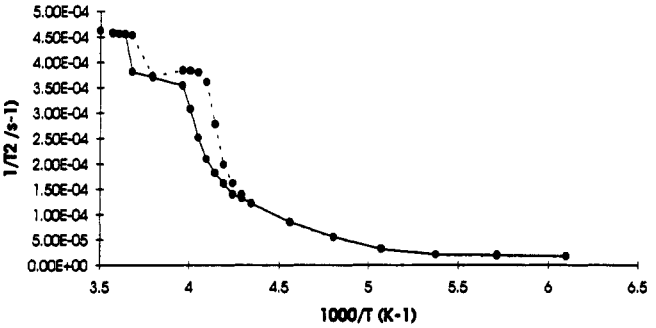

Figure 2. Apparent spin–spin relaxation rate ($1/T_2$) of the pore water vs inverse temperature of sample A. Dotted line represents cooling of the sample. Solid line represents heating of the sample.

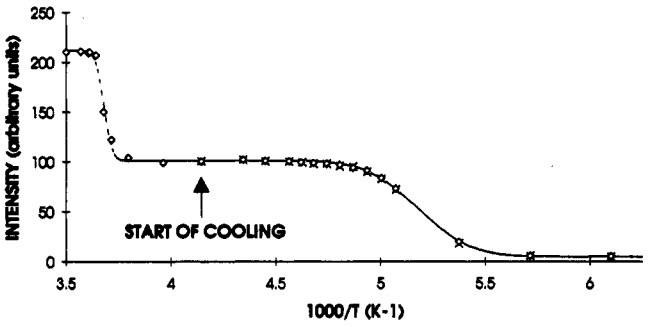

Figure 3. ^{1}H NMR signal intensity of the pore water vs inverse temperature of sample C. Solid line represents model calculations (eq A6). (×) Cooling of the sample. (◇) Heating of the sample.

discontinuities observed on cooling and rewarming), respectively. The higher temperature represents freezing of the water at the outer surface or "bulk" water which experiences no pore constraints. The lower temperature is interpreted as the freezing point of water confined in the mesopores and represents "bound" water. An additional "transition" temperature is observed at –63 °C. However, at this temperature no hysteresis effect was observed. Overloop et al.[1] have emphasized that this water does not freeze in the sense that it does not assume the structure of ice on cooling below the freezing point, and that this water exhibits a distribution of correlation times.

These same kind of characteristics are also seen in the apparent spin–spin relaxation rate ($1/T_2$) vs inverse temperature (Figure 2), although the third "transition" temperature is not well-defined in this figure. The difficulty in determining the third transition temperature from the $1/T_2$ curve is probably due to the way that these relaxation rates have been determined. No model calculations have thus been attempted in this case.

The two last mesopore systems (sample B and C) did not reveal any hysteresis effect, except for the normal freezing of bulk water at 0 °C, which is illustrated in Figure 3 for sample C. The observed "transition" temperatures (T_{c2}) were found to be –46 and –80 °C, respectively. The spin–spin relaxation rate ($1/T_2$) vs inverse

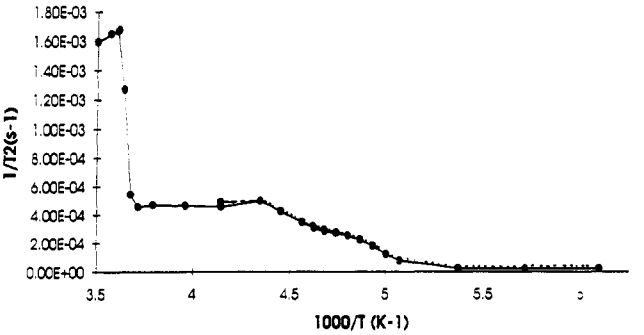

Figure 4. Apparent spin–spin relaxation rate ($1/T_2$) of the pore water vs inverse temperature of sample C. Dotted line represent cooling of the sample. Solid line represents heating of the sample.

TABLE 1: Spin–Lattice Relaxation Rate ($1/T_1$) at –10 °C and Transition Temperature Determined by a Nonlinear Curve Fit to Eq A6

sample (pore size)[a]	$1/T_1$ (s^{-1})	$\sigma(1/T_1)$ (s^{-1})	$10^3/T_{c2}$ (K^{-1})	$\sigma(10^3/T_{c2})$ (K^{-1})	correlation coeff[b]
A(38 Å)	30.84	1.44	4.149	0.008	0.99934[c,e]
			4.051	0.007	0.99987[d,e]
B(27 Å)	46.94	0.14	4.411	0.007	0.99903[c,f]
			4.413	0.007	0.99911[d,f]
C(19 Å)	85.03	4.62	5.173	0.006	0.99923[c,f]
			5.178	0.007	0.99967[d,f]
bulk water ($r = \infty$)	0.4	0.01			

[a] Pore size determined by N_2 adsorption. [b] Model fitting, eq 7. [c] Cooling of the sample. [d] Rewarming of the sample. [e] Showing hysteresis effect. [f] Showing no hysteresis. [g] σ, standard deviation

TABLE 2: Residual Water Signal Intensity (I_r) below –100 °C As Determined by a Nonlinear Curve Fit to Eq A6

sample	I_r (%)	σ
A	3.21	1.88
A[a]	2.45	0.73
B	5.98	1.02
B[a]	4.93	0.93
C	5.25	0.85
C[a]	5.58	0.99

[a] Progressive heating of the sample. σ, standard deviation.

absolute temperature shows the same kind of behavior as the intensity vs inverse temperature (Figure 4). The transition temperatures determined for the three samples are summarized in Table 1.

Even at a temperature lower than –100 °C some residual proton signal intensity (2–6%) is observable (Table 2). The origin of this signal is somewhat uncertain, but it is tempting to relate it to silanol protons on the surface of the pores, as observed by IR measurements. However, this question cannot be resolved on the basis of this study alone.

A number of theoretical and experimental works published in the past two decades, of which three are cited in the list of references,[5-7] have dealt with the relation between proton spin–lattice relaxation rate ($1/T_1$) of water confined in porous materials and the pore dimension. For the same "family" of porous materials, a simple linear relation between spin–lattice relaxation rate ($1/T_1$) and the inverse pore radius ($1/r$) has been found

$$1/T_1 = k_m(1/r) \tag{2}$$

where k_m is a constant characteristic of the porous material. Combining the well-known Kelvin equation

$$\Delta T = -\frac{2\gamma M T_0 k}{\rho \Delta H}\frac{1}{r} \tag{3}$$

(where, T_0 is the normal freezing point, ΔH the molar heat, γ surface tension, M the molecular weight, ρ the density of the adsorbate, and k the Boltzmann constant) with eq 2 suggests a

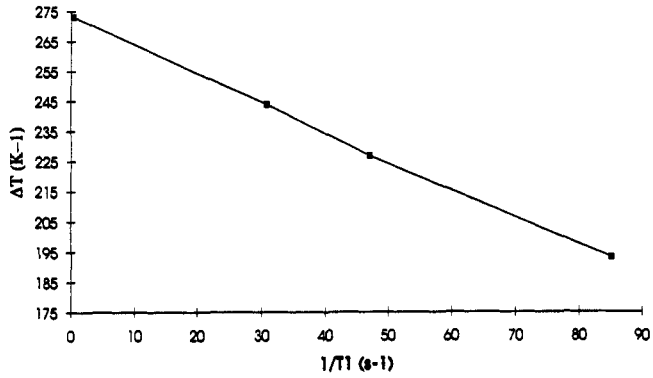

Figure 5. Lowering of the freezing point (ΔT) of pore water confined in mesopores vs spin–lattice relaxation rate ($1/T_1$).

simple linear equation between the spin–lattice relaxation rate and the lowering of the freezing point (ΔT).

The numerical data for the observed transition temperatures (<0 °C) and the spin–lattice relaxation rates of the confined water for the three mesopore systems investigated are summarized in Table 1. The spin–lattice relaxation rate for pure water ($\Delta T = 0$) is included for completeness. A plot of $1/T_1$ vs ΔT (Figure 5) reveals a linear relationship between the two parameters.

These results show an excellent internal consistency between the NMR parameters and suggests that pore size for mesopore systems can be determined by different NMR parameters: intensity, line width/spin–spin relaxation rate, and spin–lattice relaxation time.

However, it must be emphasized that only the first sample (sample A) reveals an observable hysteresis effect and thus defines unambigiously a macroscopic freezing point.

Despite the fact that only three mesopore samples have been studied in this work some interesting questions arise. Does a critical pore dimension exist at which a hysteresis effect can be observed above this critical dimension and not below, and what does this tell us about the macroscopic and colligative property of freezing? Moreover, is Kelvin's rule (eq 3) still applicable below this critical pore dimension? More insight into these matters will probably be revealed when these NMR data are correlated with N_2 adsorption and other physicochemical data. These questions will be the subject of an intensified study in our laboratory.

The advantage in using MCM-41 materials is the feasibility of preparing porous materials with well-defined and homogeneous pore dimensions as the pore size can be tailored between 16 and 100 Å. The results presented in Figure 5 indicate that the Kelvin equation can be applied to estimate the pore dimension even when no hysteresis effect is observable.

Acknowledgment. Financial support by the Research Council of Norway and Deminex Research Grant are gratefully acknowledged.

Appendix

Overloop et al.[1] have rationalized the behavior of these NMR observations by applying known models for the molecular motion in fluids and solids leading to a log-normal distribution of correlation times

$$P(\tau)\,d\tau = (1/B)\exp(-Z^2/B^2)\,dZ \quad Z = \ln(\tau/\tau^*) \qquad \text{(A1)}$$

See ref 1 for further details. However, they do not present any mathematical expression between temperature and intensity. This can be done by the following argument. Assuming[1]

$$\tau^* = \tau_0 \exp(\Delta H/RT) \qquad \text{(A2)}$$

where ΔH is the activation enthalpy of the bound water and T is the absolute temperature, and substituting eq A2 into eq A1 and defining a new variable $X = ZR/\Delta H$ (dimension of inverse temperature), eq A1 can be transformed to

$$P(\tau)\,d\tau = (1/B')\exp(-X^2/B'^2)\,dX, \quad B' = BR/\Delta H \qquad \text{(A3)}$$

Integrating eq A3 from $\tau = 0$ to a critical correlation time τ_c, the intensity of the NMR signal (I) as a function of the inverse absolute temperature (X) can be written:

$$I(X) = \int_0^{\tau_c} P(\tau)\,d\tau = (1/B')\int_{-\infty}^{X-X_c} \exp(-X^2/B'^2)\,dX,$$
$$X_c = 1/T_c = R\ln(t_c/\tau_0)/\Delta H \qquad \text{(A4)}$$

B' gives information on the width of the distribution function. The integral on the right-hand side of eq A4 is identical to the so-called error function (erf), implying that the normalized intensity of the NMR signal vs the inverse temperature X can be written:

$$I(X) = 1 - \mathrm{erf}(X - X_c) \qquad \text{(A5)}$$

If more than a single critical temperature X_c exist, eq A5 can be generalized

$$I(X) = A_0 - \sum_i A_i\,\mathrm{erf}(X - X_{ci}) \qquad \text{(A6)}$$

where A_0 and A_i represent intensities. Each transition is further characterized by a line width (B') which is related to the width of the distribution of correlation times B in eq A1 by $B = \Delta H(B'/R)$. One should keep in mind that in the case of a thermodynamic phase transition, eq A6 is not strictly valid, because a phase transition involves a discontinuity in the correlation time τ at the transition temperature. However, we believe that the idea of defining a critical correlation time τ_c and integrating the correlation distribution function up to this limit also gives an adequate description of the phase transition behavior.

The observed NMR intensities vs inverse temperature (1000/T) are fitted to the generalized function given by eq A6.

References and Notes

(1) Overloop, K.; Van Gerven, L. *J. Magn. Reson. Ser. A* **1993**, *101*, 179.
(2) Kresge, C. T.; Leonowics, M. E.; Roth, W. J.; Vartuli, J. C.; Beck, J. S. *Nature* **1992**, *359*, 710.
(3) Beck, J. S. et al. *J. Am. Chem. Soc.* **1992**, *114*, 10834.
(4) Beck, J. S. et al. (Mobil Oil Co.) **1991**, US-A 5057296; **1992**, US-A 5108725. Kresge, C. T. et al. (Mobil Oil Co.) **1992**, US-A 5098684; **1992**, US-A 5102643.
(5) Gallegos, D. P.; Munn, K.; Smith, D. M.; Stermer, D. L. *J. Colloid Interface Sci.* **1982**, *119*, 127.
(6) Brownstein, K. R.; Tarr, C. E. *J. Magn. Reson.* **1977**, *96*, 17.
(7) Glasel, J. A.; Lee, K. H. *J. Am. Chem. Soc.* **1974**, *96*, 970.